

Flame Synthesis of Nanostructured Sorbents for Desulfurization in Fuel Cells

Osifo Akhemonkhan, Ranjan K. Pati, Sicong Hou and Sheryl Ehrman
Dept. of Chemical Engineering, University of Maryland, College Park, MD, 20742

Charles Rong and Deryn Chu
Army Research laboratory, Adelphi MD, 20783

Abstract:

In the present study, high surface area sorbents for desulfurization in fuel cells are produced using the flame spray pyrolysis (FSP) method. The flame synthesis process offers a single step method for preparation of these oxides while retaining good particle qualities. The process involves the atomization of precursor solutions, here metal acetates and nitrates, which are then passed over a methane, oxygen and nitrogen flame and then collected by thermophoresis. The sorbents produced are mixed oxides, and include CuFe_2O_4 , CuAl_2O_4 , CuCr_2O_4 , CuO/CeO_2 . Mixed oxides such as CuFe_2O_4 , CuAl_2O_4 , and CuCr_2O_4 in the spinel phase (AB_2O_4) have higher sulfur removal efficiencies because the reduction of Cu to Cu metal in these oxides is much slower (copper is retained in the Cu^{2+} and Cu^{1+} oxidation states) than in single oxides. CuO/CeO_2 does not form the spinel structure but CeO_2 retains Cu in its cluster, preventing its reduction to a metal state. The particles produced using FSP are characterized using thermogravimetric analysis (TGA) to determine the impurities in the particles, X-ray diffraction (XRD) for phase analysis and crystal structure determination, BET gas absorption surface area to determine the surface area and transmission electron microscopy (TEM) for particle size morphology and of the material. The surface area of the particles produced ranged from 38 - $157\text{m}^2/\text{g}$. XRD analysis of the particles indicated the formation of the fluorite phase of CeO_2 , for the CuO/CeO_2 particles, with no indication of the formation of a separate copper oxide phase. XRD analysis of the particles shows the

formation of spinel phase with the presence of individual oxides. Pure spinel phase of these materials can be obtained by heat treatment.

Introduction:

Fuel cells are electrochemical devices that convert chemical energy to electrical energy. Each side of a fuel cell has an electrode (cathode and anode). Fuel e.g. hydrogen is diffused to the anode where it is oxidized and dissociates into protons and electrons. The protons flow to the cathode through the electrolyte while the electrons, required for the reduction reaction at the cathode, flow through an external circuit thus supplying power. Fuel cells unlike the standard energy devices currently used, e.g. heat engines, offer a more efficient and environmentally friendly way of producing energy. Energy from fuel cells is produced without combusting fossil fuels that emit harmful gases into the atmosphere furthermore, its maximum efficiency is independent of the carnot cycle principle allowing it to be more productive than traditional power devices such as gas turbines and combustion engines [4]. Fuel cells are generally categorized by their electrolytes i.e. the material between the two electrodes. Proton Exchange Membrane (PEM) and Solid Oxide (SOFC) fuel cells are two of the different types of fuel cells that show great potential as substitutes for traditional power devices others include Alkaline (AFC), Phosphoric Acid (PAFC), Molten Carbonate (MCFC).

The ideal fuel of PEMs and SOFCs is pure hydrogen, but because of the lack of distribution infrastructure and storage methods, on site or on-board production of hydrogen is considered to be the most promising way for using stationary and mobile fuel cell systems. Natural gas

produced from petroleum can be reformed to produce hydrogen. During the reforming process hydrogen sulfide (H_2S) and sulfur dioxide (SO_2) poison the steam reforming catalysts and are released into the atmosphere. The presence of these sulfur compounds in the raw materials shortens the reforming process. These compounds are removed at high temperatures ($600-800^\circ C$) through the process of desulfurization.

However, desulphurization technology is most efficient when it is applied with sorbents, which can effectively remove sulfur compounds like H_2S and SO_2 . Sorbents should have effective sulfur loading capacity, high H_2S removal efficiency and should be easily regenerable. Various types of sorbents have been developed over past years most of which are either single or mixed metal oxides e.g. ZnO , CuO , Cu_2O , Zn_2TiO_4 and $ZnFe_2O_4$ [11,2]. However during the desulfurization process the ZnO based sorbents separate into individual oxide components and subsequently ZnO reduces to elemental Zn at high temperatures [5]. The CuO sorbent though having the highest H_2S removal efficiency amongst the single metal oxides, is also reduced to metallic Cu by H_2 and CO , this lowers its overall desulfurization efficiency. Combining CuO with other oxides like chromium oxide (Cr_2O_3), cerium oxide (CeO_2), aluminum oxide (Al_2O_3) and ferric oxide (Fe_2O_3) can retain the copper at +2 or +1 oxidation states [2,24,25,26]. The resulting oxides formed have the spinel structure, which is more thermodynamically stable and has a slower reaction rate than its individual component oxides. Binary oxides have been reported to have sulfur removal efficiencies as high as 99% and complete conversion of CuO at $750^\circ C$. These sorbents were produced by sol-gel, co-precipitation and hydrothermal methods. In this experiment the synthesis and characterization of nanosized and high surface area $CuFe_2O_4$, $CuAl_2O_4$, $CuCr_2O_4$, CuO/CeO_2 with a single step flame spray pyrolysis method is reported. The process involves the pyrolysis of aqueous solutions of the metal

nitrate without addition of any extra fuel in the methane oxygen flame.

Experimental:

The precursors used for making the sorbents are copper (II) nitrate trihydrate, Iron (III) nitrate nonahydrate, cerium (III) acetate hydrate, chromium (III) acetate, copper (II) acetate monohydrate, chromium (III) nitrate nonahydrate, aluminum nitrate nonahydrate and cerium (III) nitrate hexahydrate. A series of 0.3 molar aqueous precursor solutions have been made with deionized water and mixed in the stoichiometric ratio for the preparation of CuFe_2O_4 , CuAl_2O_4 , CuCr_2O_4 , CuO/CeO_2 . For CuO/CeO_2 , some additional solutions have been made with $\text{CuO}:\text{CeO}_2$ mole ratios 1:1, 1:3, 2:3, 3:2 and 3:1. The solutions are then atomized with the help of compressed air in a medical nebulizer. The droplets from the nebulizer are then sent directly into a flame reactor. The flame in the reactor is generated with methane, oxygen and nitrogen gases. The total flow rates for each gas including the contributions from the air used to atomize the precursor were methane 0.90 l/min, oxygen 2.61 l/min and nitrogen 5.95 l/min. The maximum temperature of the flame using these flowrates was in the range of 1400 - 1500°C, which was measured by using S-type (Pt/10%Rh-Pt) thermocouple. In the reactor, the droplets undergo a series of physical and chemical steps including solvent evaporation and precipitation, intraparticle reaction and densification, to form the final product - a dense particle. The particles move from the reactor to a water-cooled surface placed directly over the reactor. The temperature gradient caused by placing the cooled surface above the flame reactor causes the particles to move from a hotter region to the cooler surface - a thermophoresis process. The same sorbent materials have been made by coprecipitation method using metal nitrate and sodium hydroxide (coprecipitation agent) to compare the materials from flame synthesis process. After coprecipitation, the metal hydroxide precipitates are filtered and washed thoroughly with deionized water. The

precipitated are then dried and calcined at different temperatures starting from 650°C to 950°C

The synthesized materials were then characterized by powder X-ray diffraction (XRD) using $\text{CuK}\alpha$ ($\lambda = 1.5408\text{\AA}$) incident radiation for the phase analysis and crystal structure determination. The Brunauer, Emmett and Teller (BET) gas absorption method was applied to investigate the surface area of the sample. Transmission electron microscopic (TEM) imaging was used for the particle size analysis and surface morphology of the material. The activity i.e. sulfidation and sulfur removal efficiency of the sorbents produce were investigated using a small plug flow reactor. Gas chromatography was used to quantify the concentration of products. To determine the reaction rate, measurements were made of H_2S and SO_2 conversion as a function of the partial pressures of the reactants and products, $\text{H}_2\text{S}/\text{SO}_2$ and elemental sulfur. Catalyst performance was determined by generating conversion profiles as a function of temperature under realistic desulfurization conditions. Temperatures used were up to 800°C.

Results and Discussion:

X-ray diffraction patterns of as prepared and CuO/CeO_2 are shown in figure 1. Figure 1(a) represents the diffraction pattern of CuO/CeO_2 particles before undergoing the desulfurization process, which shows the presence of both CuO and CeO_2 . Figure 1 (b) represents the diffraction pattern of the same material after the desulfurization reaction. It is seen in figure 1(b) that there is no peak corresponding to CuO and the formation of CuS during the desulfurization reaction, which suggests that CuO is converted to CuS during the desulfurization process [2]. X-ray diffraction pattern of as prepared CuO/CeO_2 prepared by coprecipitation method shows amorphous nature, which becomes crystalline upon heat treatment of the sample at a temperature of 650°C. As the calcination temperature increases (600–950°C), the diffraction peaks get sharpened

because of the increase in crystallite size. Diffraction patterns of flame synthesized CuFe_2O_4 and CuAl_2O_4 (not shown here) shows the presence of a mixture of individual oxides and spinel, however the coprecipitated as prepared CuFe_2O_4 and CuAl_2O_4 samples are amorphous in nature, and only show crystallinity after calcinations of the sample. A mixture of phase is obtained for CuAl_2O_4 sample upon calcinations at temperature as high as 950°C . This suggests that calcination at higher temperature is needed to get the pure spinel phase.

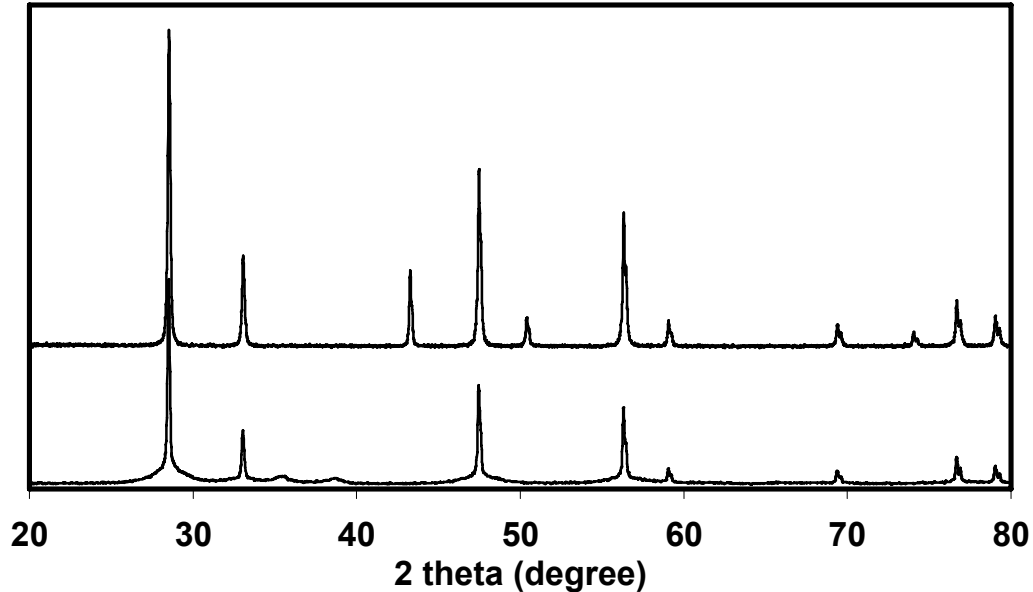


Figure 1: X-ray diffraction study of flame synthesized (a) as prepared CuO/CeO_2 sample and (b) CuO/CeO_2 sample after desulfurization reaction

Figure 2a shows transmission electron microscopic image of flame synthesized CuO/CeO_2 with $\text{CuO} : \text{CeO}_2$ mole ratio 2:3. The particles are nearly spherical in shape and have a size in the range of 3-5nm. The absence of bigger particles (greater than 100 nm) suggests that the precursor droplets are vaporized completely in the flame and that the particles

form by gas-to-particle conversion following reaction of the precursor species to form metal oxides.

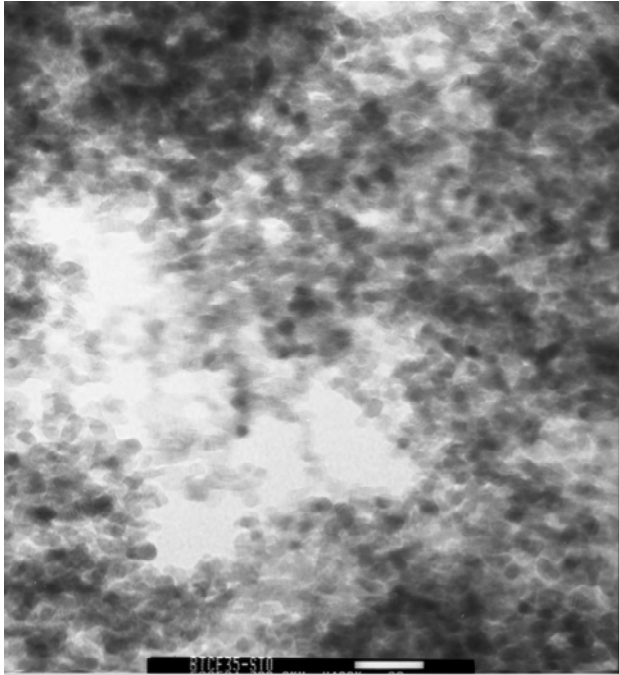


Figure 2a:
Transmission
electron micrograph
and selected area electron diffraction (SAED) pattern of
 CuO/CeO_2 with $\text{CuO} : \text{CeO}_2$ ratio 2:3.

Table 1 shows the results from BET surface area analysis and XRD diffraction studies. It shows a comparison between the particles created by co-precipitation and particles synthesized by spray pyrolysis. From the table it can be seen that flame synthesized particles have on average, a greater surface area as expected.

Table 1- Results from BET surface area analysis and XRD diffraction studies

Samples	BET surface area (m ² /g)	
CuO/CeO ₂ (flame)		157
CuO/CeO ₂ (co-prec)		-
CuO/CeO ₂ (co-prec) (650°C)		52
CuO/CeO ₂ (co-prec) (650°C)		13.5
CuO/CeO ₂ (co-prec) (650°C)		0.5
CuO/Al ₂ O ₃ (co-prec)		55
CuO/Al ₂ O ₃ (co-prec) (650°C)	42	
CuO/Al ₂ O ₃ (co-prec) (800°C)		25
CuO/Al ₂ O ₃ (co-prec) (950°C)		3
CuO/Fe ₂ O ₃ (flame)		52
CuO/Cr ₂ O ₃ (flame)		38
CuO/Cr ₂ O ₃ (co-prec)		-
CuO/Cr ₂ O ₃ (co-prec) (650°C)		1.27

Desulfidation reactions of synthesized sorbents were conducted at temperatures up to 800°C. Table 2 shows results from sulfidation tests of CuFe₂O₄, CuO/CeO₂, CuAl₂O₄, CuO/CeO₂. All sorbents tested had high H₂S removal efficiencies - over 95% and relatively high sulfidation capacities. Flame synthesized CuO/CeO₂ particles maintained a higher surface area and had a higher sulfur loading capacity than CuO/CeO₂ particles created by co-precipitation. From the result it is clear that surface area plays a big role in desulfurization process. CuFe₂O₃ sample has lowest sulfidation capacity because Fe₂O₃ is reduced to Fe in the reducing environment during the desulfurization reaction.

Table 2- *desulfidation test results of CuFe₂O₄, CuO/CeO₂, CuAl₂O₄, CuO/CeO₂ made by flame synthesis and coprecipitation method*

Sample	Sulfidation capacity at BET (m ² /g) 30ppm breakthrough at (at 800°C) 800°C (g S/g sorbent)	Efficiency of H ₂ S Desorbed/adsorbed	
CuFe ₂ O ₄ (Flame Synthesized)	6.2	96%	-
CuO/CeO ₂ (coprecipitated)	10.4	98%	13.5
CuAl ₂ O ₄ (coprecipitated)	12.3	99%	24.9
CuO/CeO ₂ (flame synthesized)	12.4	98%	33.5

Summary and Conclusion:

Flame synthesis is an easy, single step method for the preparation of CuFe₂O₄, CuAl₂O₄, CuCr₂O₄, CuO/CeO₂ powder. The process is shorter than most wet chemical methods and is cost efficient. The flame-synthesized sorbents have higher surface areas than particles synthesized by co-precipitation. Since the desulfurization reaction takes place on the surface of the particles, the flame-synthesized sorbents have higher sulfur loading capacities because of their higher surface area. XRD analysis of the particles indicated the formation of the fluorite phase of CeO₂, for the CuO/CeO₂ particles, with no indication of the formation of a separate copper oxide phase. XRD analysis of the particles shows the formation of spinel phase with the presence of individual oxides. Pure spinel phase of these materials can be obtained by heat treatment.

Acknowledgements:

Ranjan K. Pati and Sheryl H. Ehrman would like to thank the U.S. Army Research Laboratory for financial support and instrument usage.

References

1. Ranjan K. Pati et al. Flame synthesis of nanosized Cu-Ce-O, Ni-Ce-O and Fe-Ce-O water gas shift catalysts (submitted).
2. Z. Li, M. Flytzani-Stephanopoulos, *Ind. Eng. Chem.* 36 (1997) 187-196
- T. Zhu, A. Dreher, M. Flytzani-Stephanopoulos, *App. Catal. B.* 21 (1999) 103-120.
3. S. Ehrman. Study of structure processing relationship in multi-component oxides formed by spray pyrolysis. Proposal to the Petroleum Research Foundation.
4. A. Faghri, Z. Guo, *International Journal of Heat and mass Transfer*, 48 (2005) 3891-3920.
5. R. Slimane, J. Abbasian, *Advances in Environmental Research*, 4 (2000) 147-162
6. T. Zhu, A. Dreher, M. Flytzani-Stephanopoulos, *Appl. Catal. B* 21 (1999) 103-120
7. T. Kyotani, H. Kawashima, A. Tomita, A. Palmer, E. Furimsky, *Fuel* 68 (1989) 218- 223
8. W. Liu, and M. Flytzani-Stephanopoulos, *J. Catal.* 153, (1995) 304
9. L. Kundakovic and M. Flytzani-Stephanopoulos, *J. Catal.* 179 (1998) 203-221
10. S. Lew, K. Jothimurugesan, M. Flytzani-Stephanopoulos, *M. Ind. Eng. Chem. Res.* 28 (1989) 535-541
11. S. Lew, M. Flytzani-Stephanopoulos, A. Sarofim, *Chem. Eng. Sci.* 47 (6) 1992 1421-1431
12. S. Lew, A. Sarofim, M. Flytzani-Stephanopoulos, *Ind. Eng. Chem. Res.* 31 (1992) 1890-1899
13. K. Otsuka, T. Ushiyama, I. Yamanaka, *Chem. Lett.* (1993) 1517
14. J. Y. Ying and A. Tschöpe, *Chem. Eng. J.* **64**, 225 (1996).
15. T. Johannessen, J. R. Jenson, M. Mosleh, J. Johansen, U. Quaade, and H. Livbjerg: *Chem. Engng. Res. & Design* **82**, 1444 (2004).
16. L. Madler, W. J. Stark, and S. E. Pratsinis. *J. Mater. Res.* **17**, 1356 (2002).
17. J. Kaspar, P. Fornasiero, and M. Graziani *Catal. Today* **50**, 285 (1999).

18. P. Bera, S. T. Aruna, K. C. Patil, and M. S. Hegde *J. Catal.* **186**, 36 (1999).
19. Y. C. Zhou and M. N. Rahaman: *J. Mater. Res.* **8**, 1680 (1993).
20. A. Tschöpe, W. Liu, M. Flytzani-Stephanopoulos, and J. Y. Ying *J. Catal.* **157**, 42 (1995).
21. A. Trovarelli *Catal. Rev.-Sci. Eng.* **38**, 439 (1996).
22. I. C. Lee, R. K. Pati, S. H. Ehrman, and D. Chu, *Catal. Letters.*, (2005, submitted).
23. M. Suzuki, M. Kagawa, Y. Syono, and T. Hirai: *J. Mater. Sci.* **27**, 679 (1992).
24. M. Flytzani-Stephanopoulos, G.R. Gavalas, M. Bagajewicz, S.S. Tamhankar. *Ind. Eng. Chem. Res.* **28**, (1989) 931-940
25. G.R. Gavalas, V. Patrick, *J. Am. Ceram. Soc.* **73**, (1990) 358-369
26. G. Sick, K. Schwerdtfeger, *Metall. Trans.* **18B** (1987) 603-609